EAI Endorsed Transactions
on Energy Web
Research Article EAI.EU

Research on Active Equalization of Energy Storage Lithium Batteries under a Modular Layered Architecture for Smart Grid Applications

Qingdong Luo[1,*], Xiyuan Wan[1], Qiangwei Liu[2], Jingjing Lou[1], Zhikang Jin[1] and Chaoqun Jin[1], Pengfei Zhen[3]

[1]Yiwu Industrial and Commercial College, Yiwu, China, 322000
[2]Ningbo Henghui Electrical Co., Ltd, Ningbo, China, 315103
[3]Taizhou Vocational & Technical College, Taizhou, China, 318000

Abstract

INTRODUCTION: In smart grid applications, energy storage systems (ESS) are critical for balancing power supply and demand, but they often suffer from performance degradation due to State of Charge (SOC) inconsistencies in series-configured lithium battery packs. These disparities can compromise grid stability and battery lifespan.
OBJECTIVES: This study proposes an active equalization method based on a novel modular layered architecture for ESS in smart grids. The core innovation lies in the synergistic combination of a hierarchical bidirectional Buck-Boost topology and a multivariable fusion fuzzy logic control strategy, aiming to enhance battery consistency, efficiency, and reliability for grid support.
METHODS: A hierarchical BUCK-BOOST-based circuit is designed to enable bidirectional energy transfer, incorporating a multivariable fuzzy controller for real-time regulation of balancing currents. This approach facilitates cooperative equalization within and between battery groups, optimizing energy flow.
RESULTS: Simulations based on an eight-cell model in Matlab/Simulink demonstrate that the proposed hierarchical topology reduces equalization time by 11.53% compared to the conventional single-layer topology. Furthermore, with the proposed multivariable fusion fuzzy logic control algorithm, the equalization time is further reduced by 26%, significantly improving both the equalization speed and adaptability to dynamic grid conditions.
CONCLUSION: The proposed strategy effectively mitigates battery inconsistencies, enhancing the overall performance and safety of energy storage systems in practical applications. It provides a reliable technical approach for battery management in smart grids.

Keywords: Energy storage lithium battery, State of charge (SOC), Active equalization, Hierarchical equalization circuit, Fuzzy control

Received on 27 January 2026, accepted on 31 March 2026, published on 07 May 2026

doi: 10.4108/ew.11711

*Corresponding author. Email: autodd@126.com

1. Introduction

In smart grid applications, large-scale energy storage systems (ESS) fundamentally rely on series-configured lithium-ion battery packs to achieve the required high operating voltages and capacities. However, as the number of cells increases, inconsistency issues within the battery pack become significantly pronounced, critically constraining the system's

operational safety, cycle life, and overall efficiency [1-3]. For grid-scale ESS, which undertakes critical functions such as peak shaving, frequency regulation, and renewable energy integration, battery inconsistency can lead to reduced available capacity, accelerated system degradation, and potential safety hazards, thereby impacting the stability and economy of grid operations. Cell-to-cell variations, manifested as discrepancies in key parameters such as capacity, voltage, internal resistance, and State of Charge (SOC), are inevitable in mass-produced batteries. Significant inconsistencies can critically compromise pack safety and reduce service life [4-5]. Under standard operating conditions, the interplay between intrinsic and extrinsic factors with operational parameters renders heterogeneity unavoidable. Equalization control aims to confine cell-to-cell variations within a defined threshold, reduce inter-cell discrepancies, and thereby enhance the service life of lithium batteries[6-7].

The key issues in equalization primarily involve equalization topologies design and equalization strategies develop [8]. Equalization strategies mainly refer to balancing modes, energy transfer methods, battery charging priority, equalization activation timing, etc. Based on the differences in energy transfer methods of lithium batteries, lithium battery equalization is categorized into passive and active balancing [9].

Passive balancing employs a resistor connected in parallel with a battery cell's electrodes, where the balancing mechanism is activated by toggling a switch associated with the resistor. When the capacity of a specific battery cell exceeds a preset equalization threshold, the switch is closed, allowing excess electrical energy to be dissipated through the resistor, thereby achieving state balance among battery cells [10]. Passive balancing is characterized by simple implementation and low design cost, but the phenomenon of resistor heating during the balancing process conflicts with the goal of improving balancing speed.

Active balancing relies on specific circuit components to construct balancing networks, effectively transferring excess battery energy to other battery cells [11]. Based on the type of energy storage components, it is generally classified into inductor-based, capacitor-based, transformer-based, and converter-based balancing.

The advantage of the inductance balancing strategy is that it does not rely on the voltage difference between adjacent batteries, ensuring that a balancing current can be output even under a small voltage difference, effectively carrying out the balancing task. Venkatasatish et al. developed an inductor-based cell balancing unit that significantly reduces the number of power switches, thereby simplifying the circuit design and enhancing the system's reliability and cost-effectiveness[12]. Capacitor balancing relies on the inter-cell voltage disparity and the inherent energy storage properties of capacitor to achieve the purpose of energy transfer. Its advantages mainly include: good voltage consistency, relatively simple control strategy, and easy system expansion, etc. [13]. However, the equalization rate of the capacitor-based circuit is constrained by the interdependency of capacitive properties and inter-cell voltage disparities; specifically, the equilibration velocity diminishes progressively as the voltage differential narrows. Therefore, capacitor balancing is not suitable for energy storage systems with high-precision and high-balancing speed requirements. Transformer balancing belongs to isolated balancing, with its circuit configurations typically categorized into multi-winding and single-winding architectures. The multi-winding transformer configuration incorporates a single primary winding and multiple secondary windings, enabling efficient energy exchange between individual battery cells and the integrated battery pack. In the single-winding structure, under imbalanced battery conditions, the transformer's primary winding switch is activated, enabling surplus energy to be relayed from the primary to the secondary winding via mutual inductance. This mechanism ensures redistribution of redundant energy from individual cells to the entire battery assembly. Reference [14] proposed a combined forward and flyback transformer balancing structure. Under conditions of significant voltage disparity within a battery pack, the forward mode is employed for equalization; conversely, for minor voltage differences, balancing is accomplished through dual flyback conversion operations; when the batteries to be balanced are in different packs, a single flyback conversion is used for balancing. This structure realizes energy conversion between any individual battery cells, but it is primarily suitable for small-scale battery packs, limiting its application in large-scale grid energy storage systems requiring long battery strings. Reference [15] proposed a transformer modular balancing topology, which improves the scalability of the balancing circuit. The internal part uses a flyback transformer for balancing, while the inter-module part uses an upper-level transformer for balancing. The advantage of this topology is that the internal and external operations of the module are independent and can work simultaneously, with multiple energy transfer paths and high balancing efficiency. However, the physical dimensions and implementation costs of the equalization system exhibit a proportional expansion as the quantity of batteries requiring balancing grows. Balancing through conversion circuits is achieved by various DC/DC conversion circuits to transfer battery energy. Reference [16] proposed a hybrid balancing circuit architecture that combines a Cuk converter with a Buck-Boost converter and uses an LC resonant network to replace the traditional switch capacitor, effectively reducing the voltage stress on power devices. Reference [17] proposed an equalization scheme employing an isolated bidirectional full-bridge converter. This configuration ensures electrical isolation with state-of-charge (SOC) balancing as the primary control objective, enabling bidirectional energy transfer among battery packs. The high-frequency transformer-coupled, bidirectional active full-bridge configuration demonstrates capabilities in handling both AC and DC power conversion, making it well-suited for high-efficiency equalization demands of large-capacity battery packs in energy storage systems [18].

The efficacy of battery pack equalization is collectively determined by three critical factors: the balancing variables characterizing the internal energy states of batteries, the topological configuration governing system complexity and

reliability, and the control strategy dictating equalization efficiency [19-21]. While existing studies have established the individual roles of these factors, synergistic optimization strategies to enhance overall balancing performance demand further investigation. Furthermore, although balancing velocity exhibits strong correlation with equalization current, practical constraints imposed by operational conditions and intrinsic battery properties limit the discharge current. Consequently, identifying the optimal trade-off between balancing speed and current intensity represents a key direction for future research.

Considering the above factors, this paper designs a hierarchical BUCK-BOOST bidirectional equalization architecture and a multivariable equalization strategy fusing voltage and state of charge (SOC). This design adopts a hierarchical progressive structure: the basic layer takes two adjacent battery cells as the minimum equalization unit, and realizes fast energy exchange through a dedicated balancing module; multiple basic units are combined into upper-layer equalization units through the same architecture, so as to achieve modular expansion of the system. The balancing circuit controls the switching states of switching tubes through a multivariable fusion fuzzy logic algorithm to regulate the balancing current, consequently enabling optimized management of both balancing velocity and efficacy for energy storage lithium battery packs.

It is worth noting that the performance of any active equalization system is highly dependent on accurate and robust state estimation, particularly for State of Charge (SOC) and State of Health (SOH). Recent advancements in data-driven and machine learning methods, such as optimized Long Short-Term Memory (LSTM) networks [24, 25] and advanced electrochemical-thermal coupled models [26], have shown great potential in providing precise state information under complex operating conditions. These estimation techniques are complementary to the equalization topology and control strategy proposed in this work, and can be integrated to form a more comprehensive and intelligent Battery Management System (BMS). The focus of this paper, is on the hardware architecture and the high-level control strategy for energy redistribution.

2. Active Balancing topology design

2.1 Balancing Circuit Topology

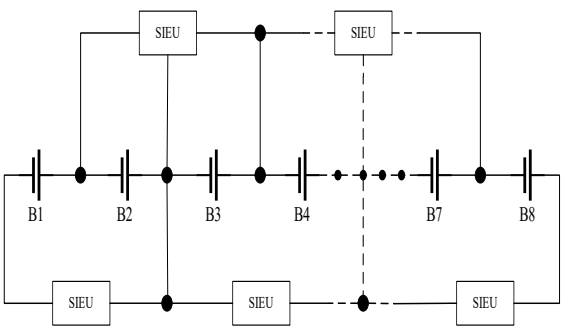

Figure 1. Illustrates the conventional single-layer Buck-Boost converter-based equalization circuit

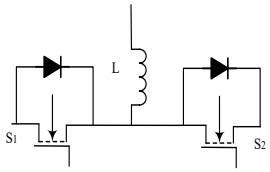

Figure 2. Single Inductor Equalization Unit (SIEU)

In Fig.1: B1~B8 are 8 lithium batteries; The single inductor equalization unit (SIEU) shown in Fig.2 represents the fundamental building block of the balancing system, where L denotes the power inductor while S1 and S2 correspond to the power switching MOSFETs.

Within the equalization configuration illustrated in Fig.1, direct energy transfer is achieved via the balancing inductor when the charge level of battery B1 exceeds that of its adjacent counterpart B2. However, for energy equalization between non-adjacent battery cells (such as B1 and B8), it is necessary to carry out gradual energy transfer through intermediate batteries (B2 to B7). Under such extreme operational scenarios, when the count of batteries engaged in energy transfer is maximized, the system experiences a substantial degradation in equalization efficacy, a noticeable decrease in balancing velocity, and a consequent compromise in overall equalization precision. This cascaded energy transmission mode has become the main bottleneck restricting system performance.

To address the problem of low equalization efficiency in series-connected battery packs, this paper designs a hierarchical BUCK-BOOST bidirectional equalization architecture, and its specific implementation scheme is shown in Fig.3. The design adopts a hierarchical progressive structure: the basic layer (marked by a green frame) takes two adjacent battery cells as the minimum equalization unit, and realizes fast energy exchange through a dedicated equalization module; multiple basic units are combined into upper-layer equalization units through the same architecture to achieve modular expansion of the system. In terms of topology construction strategy:

1) When the total number of batteries n satisfies being a power of 2, a complete binary tree structure is directly adopted for hierarchical design;

2) For the case where n is an even number but does not satisfy the power-of-2 condition, a binary recursive grouping method is adopted until the number of batteries in each group is an odd number;

3) When n is an odd number, the standard hierarchical design is preferentially implemented for the first n - 1 battery cells, and the terminal battery is connected to the previous cell through an additional single-layer equalization circuit.

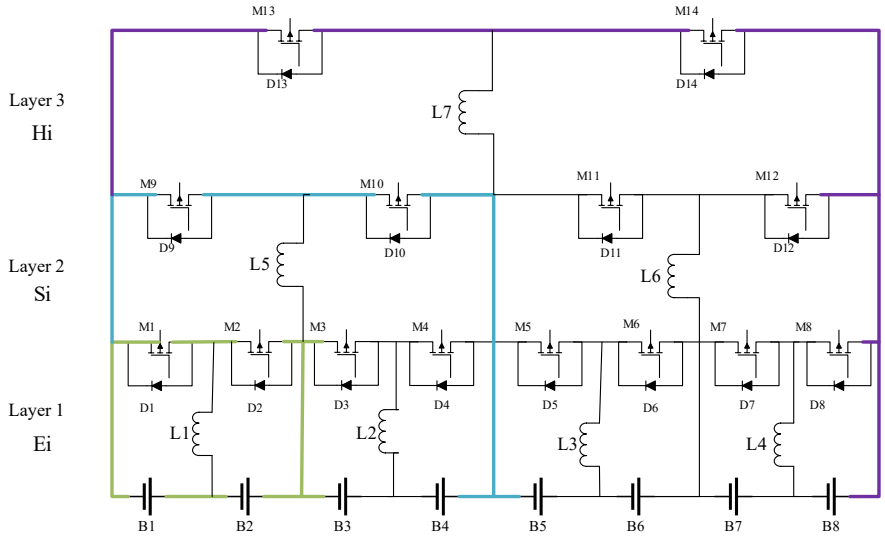

Figure 3. Hierarchical Buck-Boost circuit equalization topology

Compared with ordinary series topology, the hierarchical equalization topology can achieve equalization between non-adjacent batteries. Taking the circuit shown in Fig.3 as an example, under conditions where battery B1 exhibits a higher charge level and battery B8 a lower charge level, it is necessary to transfer the excess charge from B1 to B8 through the equalization circuit. The hierarchical equalization circuit can initiate equalization simultaneously through three layers of circuits: Layer 1 Hi, Layer 2 Si, and Layer 3 Ei, while the traditional equalization topology requires initiating equalization sequentially starting from L1 to L7. Comparatively, hierarchical equalization offers higher equalization speed. The specific working process is analyzed as follows:

B1 to B4 can be balanced with B5 to B8 through the third-layer Hi circuit. As shown in Fig.4, B1 to B4 charge and store energy in the inductor of the L7 loop, and transfer energy to B5 to B8 through the L7 loop.

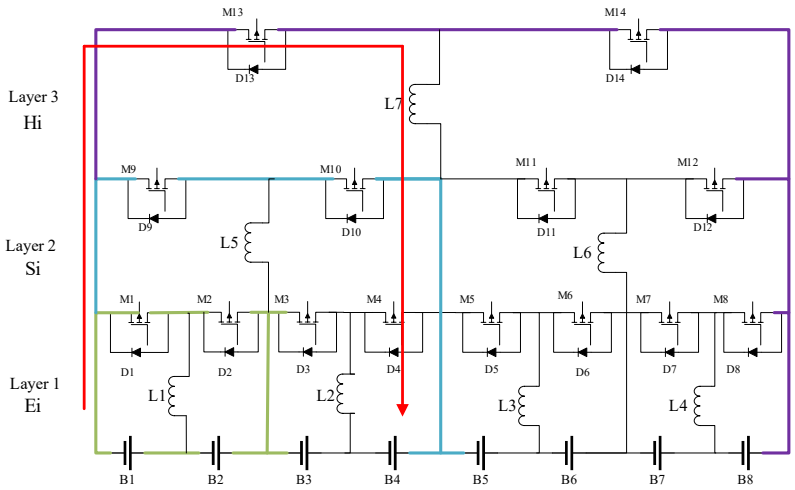

Figure 4. L7 circuit equalization

The equalization speed between the first four batteries B1-B4 and the last four batteries B5-B8 is relatively slow, failing to effectively address the issue of inconsistent state-of-charge (SoC) between B1 and B8. Therefore, it is necessary for the secondary equalization circuit Si and the primary equalization circuit Ei to operate, promoting energy transfer between B1 and B8 through energy conversion among more intra-group batteries. When the Si circuit is activated, every two adjacent

batteries form a group for inter-group equalization. It should be emphasized that the first four groups of batteries and the last four groups of batteries are only equalized through the Hi circuit, while B1, B2 and B3, B4 are only equalized through the L5 circuit. The first stage of equalization for the L5 and L1 circuits is shown in Figs. 5 and 6.

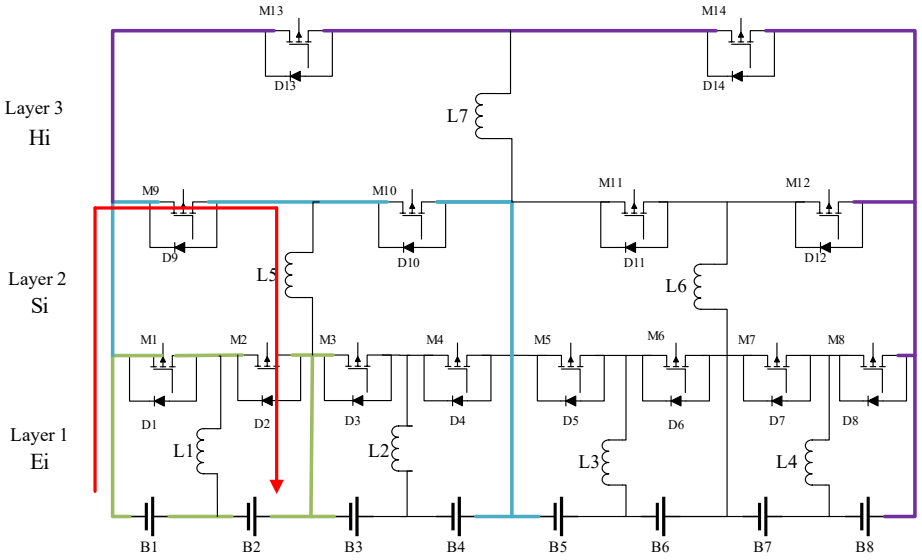

Figure 5. L5 Circuit Equalization Diagram

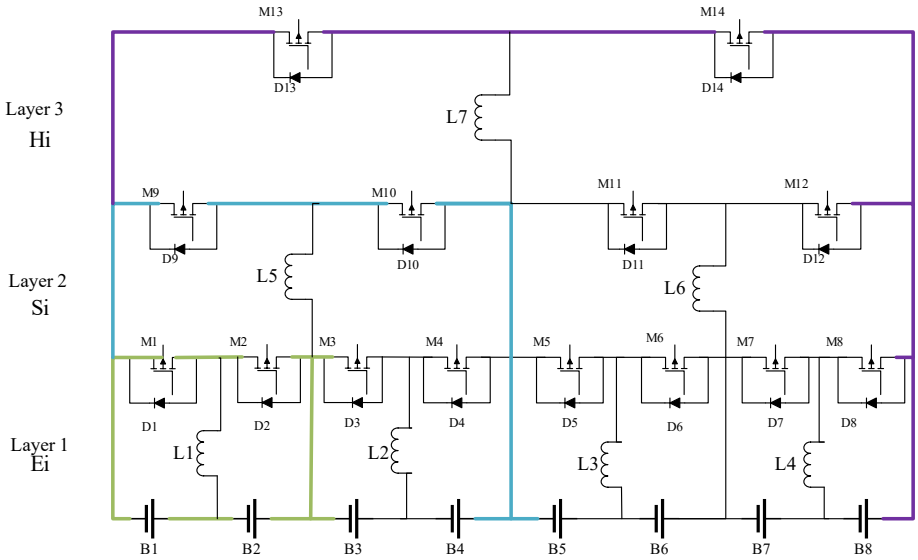

Figure 6. L1 circuit equalization diagram

After multiple above-mentioned charge-discharge cycles, excess charge is transferred through inductors, achieving intra-group battery equalization. By controlling individual cells in this manner, the equalization issue between adjacent individual cells can be resolved.

2.2 Analysis of Operating Characteristics of Equalization Circuit

The equalization module within the group is a bidirectional Buck-boost converter. Taking the intra-group equalization module L1 as an example, the bidirectional Buck-boost

equalization circuit designed for intra-group applications is presented in Figure 7.

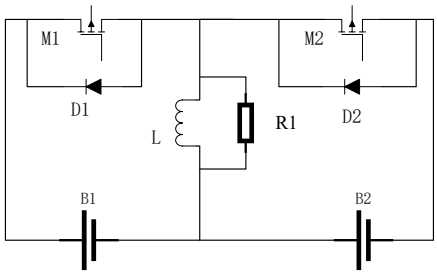

Figure 7. Buck-Boost Equalization Circuit

The circuit in Fig.7 is called an equalization unit, which is composed of control switches and energy storage components. As illustrated in Fig.7, the equalization sub-module — comprising batteries B1 and B2, inductive components, MOSFETs, and associated circuitry—facilitates bidirectional energy transfer between adjoining cells. Within this configuration, the power energy storage inductor (L) accomplishes the conversion between magnetic and electrical energy during circuit operation. R1, connected in parallel with the energy storage inductor, is a demagnetizing resistor that prevents the inductor from magnetic saturation. M1 and M2 are MOSFETs used to control the equalization on/off, and D1 and D2 are rectifier diodes. In the equalization topology circuit structure as designed in this paper, the bypass of the equalization sub-module remains unaffected by the main circuit current. Thus, regardless of the battery's operational mode—charging, discharging, or standby, it is possible to simultaneously initiate the equalization process for multiple adjacent batteries, thereby improving equalization efficiency. This paper takes the example where the charge of B1 is higher than that of B2 for illustration. When the threshold condition for activating equalization is reached, the intra-group equalization module L1 is turned on. The equalization procedure comprises two stages: B1 discharging and B2 charging.

The duty cycle of the pulse-width modulation (PWM) signal is defined as d, with a value bounded between 0 and 1, whereas T signifies the switching period of the control signal.

(1) B1 Discharging Stage

When the MOSFET M1 is turned on during 0 < t < DT, the circuit enters the discharging stage. The Kirchhoff's voltage law equation for this loop is:

$$VB_1 = i_L R_{on} + L\frac{di_L}{dt} \quad (0 < t < t_{on}) \tag{1}$$

where i_L is the current (A) , VB_1 is the voltage (V) of battery B1, L is the inductance (H) , R_{on} is the total equivalent resistance in the discharge loop, $t_{on} = DT$ is the turn-on time of M1. During the switch-on period, the discharge current can be obtained from Equation (2):

$$i_L = \frac{VB_1}{R_{on}} - \frac{VB_1}{R_{on}} e^{-t\frac{R_{on}}{L}} = \frac{VB_1}{R_{on}}(1 - e^{-t\frac{R_{on}}{L}}) \quad (0 < t < t_{on}) \tag{2}$$

When $t_{on} = DT$, the discharge current through the inductor reaches its peak value, i.e.:

$$i_L = i_{\max} = \frac{VB_1}{R_{on}}(1 - e^{-t\frac{R_{on}}{L}}) \quad (t = t_{on}) \tag{3}$$

where $i_{\max}$ is the maximum current value of the inductor. When the controller sends a control signal to turn off the MOSFET M1, the process proceeds to the next stage.

(2) B2 Charging Stage

When $DT < t < T$, the volt-ampere characteristics of the inductor determine that its current cannot change abruptly, but the voltage can change abruptly to turn on diode D2 for freewheeling, forming a charging circuit. Throughout the charging phase, the current exhibits a continuous decay, and the circuit equation for the battery charging circuit is:

$$VB_2 = R_{\text{eff}} i_L + L\frac{di_L}{dt} \quad (t_{\text{on}} < t < t_{\text{off}}) \tag{4}$$

where R_{off} corresponds to the aggregate resistance within the charging loop; VB_2 denotes the voltage of battery B2; t_{off} is the time for the current of inductor L1 to return to zero.

Obtained from (4) that:

$$i_L = i_{max}\, e^{-t-t_{\text{on}}} \frac{R_{\text{off}}}{\text{L}} - \frac{VB_2}{R_{\text{off}}}(1 - e^{-t-t_{\text{on}}})\frac{R_{\text{off}}}{L} \quad (t_{\text{on}} < t < t_{off}) \tag{5}$$

It can be seen from the above analysis that the inductor current generally changes according to the exponential function law when the inductor L is in the charging phase and discharging phase.

During both operational states (charging /discharging), R_{on} and R_{off} can be approximately ignored, Consequently, upon activation of MOSFET M1, the voltage imposed across inductor L1 equals VB1, which is the voltage of battery B1 during charging. Prior to the complete decay of the inductor current following the deactivation of MOSFET M1, the voltage sustained across inductor L1 corresponds to VB2, which is the voltage of battery B2 during discharging. The inductor current relationship is as follows:

$$i_L = \begin{cases} \frac{VB_1}{L} t & (0 < t \le t_{\text{on}}) \\ \frac{VB_1}{L} t_{\text{on}} - \frac{VB_2}{L}(t - t_{\text{on}}) & (t_{\text{on}} < t \le t_{\text{off}}) \end{cases} \tag{6}$$

The energy accumulated in the inductor can be expressed as:

$$W = \frac{1}{2} LI^2 \tag{7}$$

Where, W denotes the energy; L represents the inductance value; I is the the inductor current.

At time t_{off}, the inductor current decays to zero, which can avoid the inductor magnetic saturation phenomenon and ensure that all the magnetic energy converted from the battery during discharge is fully released. As can be seen from Equation (8):

$$\frac{VB_1}{L}t_{on} = \frac{VB_2}{L}(t_{off} - t_{on}) \tag{8}$$

Assuming T is the on-off cycle of the MOSFET, when the equalization circuit is in the discontinuous mode or critical mode, it is necessary to satisfy $t_{off} \le T$. According to Equation (8), it can be concluded that:

$$\frac{VB_1}{L}t_{on} \le \frac{VB_2}{L}(T - t_{on}) \tag{9}$$

It is derived that:

$$D \le \frac{VB_2}{VB_1 + VB_2} \tag{10}$$

It is analyzed from Equation (10) that as the inter-cell voltage disparity between adjoining battery cells diminishes, the duty cycle is set to 50%.

It is concluded from Equation (6) that:

$$i \le \frac{VB_1 DT}{L} \tag{11}$$

$$Lf \le \frac{VB_1 D}{i} \tag{12}$$

Where: T represents the control signal period; i is the equalization current; f denotes the frequency of the control signal. Given fixed values for the control signal frequency f and the inductance value L, the amplitude of the equalization current i is governed by the battery voltage VB1 and the duty cycle of the PWM signal. If the inductance value L and the control frequency f are determined, Lf should take its maximum value to ensure the stable operation of the circuit.

2.3 Simulation Verification of Equalization Circuit

This study constructs simulation models for both series-connected and hierarchical topologies of an eight-cell battery pack within the Matlab/Simulink environment, as illustrated in Figures 8 and 9. The state of charge (SOC) is selected as the balancing variable, and the equalization process employs a difference comparison algorithm. The model of the balance control strategy logic block diagrams is constructed as shown in Fig.10. The system incorporates two distinct controller types for regulating the equalization current: one for intra-group and another for inter-group balancing. These controllers share an identical topological structure and control methodology, which permits the concurrent operation of both intra-group and inter-group equalization processes. A set of three conditions is monitored in parallel, and the activation of any single condition triggers the corresponding equalization module. The balancing process terminates once the State of Charge (SOC) differential between individual cells or battery groups decreases below a predefined deactivation threshold. This hierarchical architecture facilitates synchronous balancing within and between battery groups, thereby significantly enhancing the overall equalization performance.

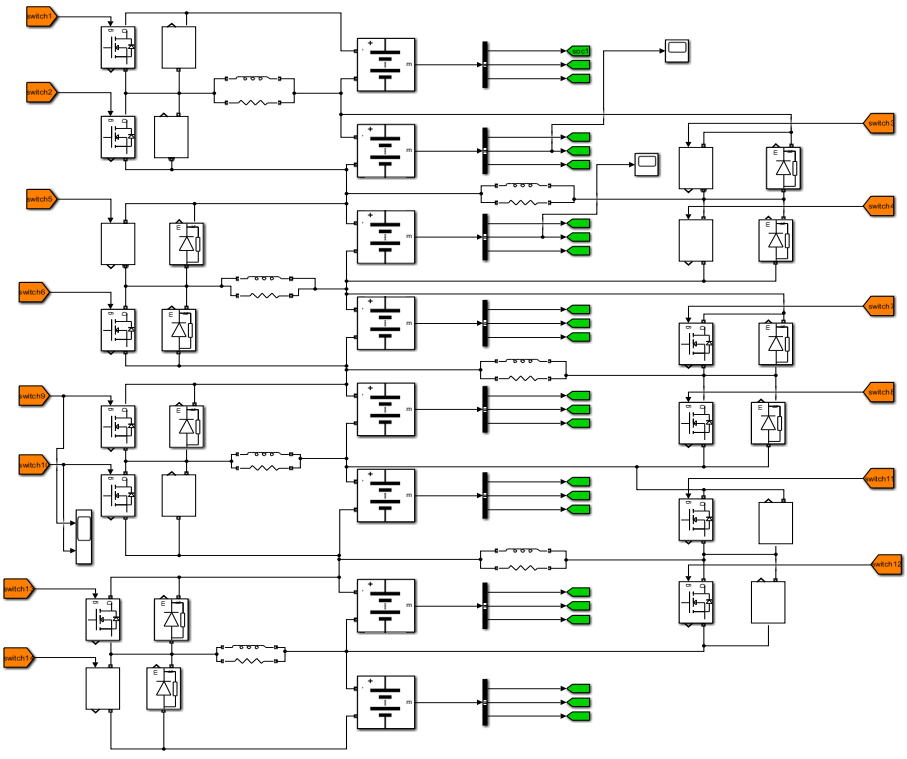

Figure 8. Simulation model of battery pack series equalization topology

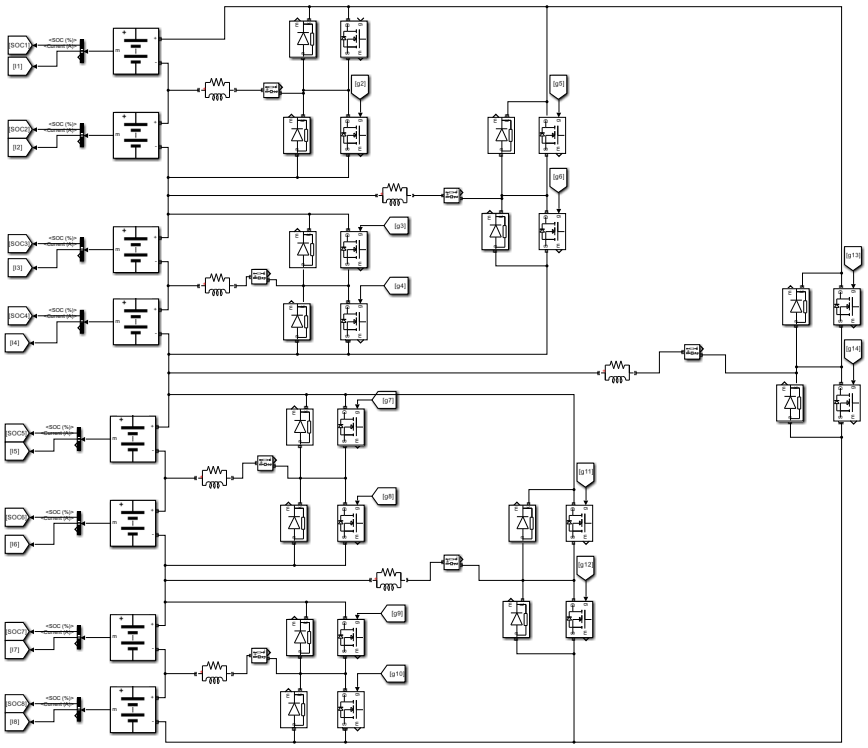

Figure 9. Simulation model of battery pack hierarchical equalization topology

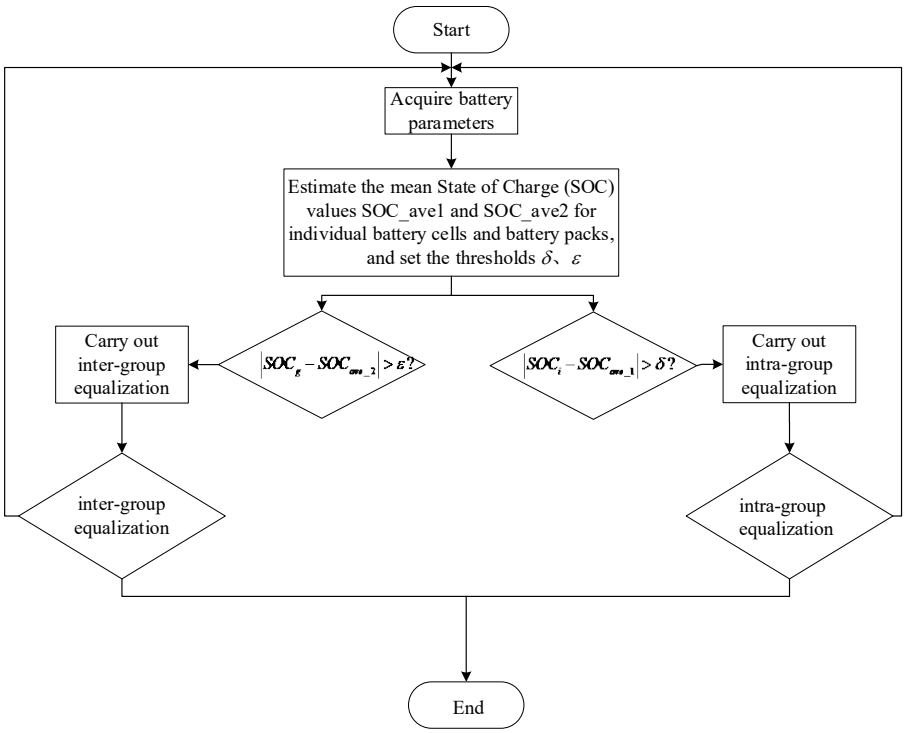

Figure 10. Equalization Process Schematic

The initial State of Charge (SOC) values are configured as: 0.65, 0.63, 0.59, 0.61, 0.57, 0.55, 0.51, 0.53; A difference comparison algorithm is employed, whereby the average SOC of adjoining cells is computed and contrasted with individual cell SOC to control the activation and deactivation of equalization.

When using a series topology for balancing, the working condition of the balancing circuit is set as follows: the equalization process is activated once the SOC discrepancy between modules exceeds 1%. The SOC estimation system determines the value relationship between adjacent single cells. If the condition $SOC_{Bi} - SOC_{Bi+1} > 0.2\%$ is met, the balancing loop starts to work until the working conditions of all loops are no longer satisfied, and the balancing process ends.

When using a hierarchical balancing topology, the working principle of the balancing circuit is the same. The system simultaneously detects whether the SOC of each bottom-level battery module and single cell meet the working conditions of Ei, Si, and Hi. If the condition of SOC(Bi) - SOC(Bi+1) > 0.2% is met, the first-level balancing circuit Ei starts to work. If [SOC(Bi) + SOC(Bi+1)] - [SOC(Bi+2) + SOC(Bi+3)] > 0.2%, the balancing circuit Si works.The high-level balancing circuit (Hi) is activated when the SOC deviation between the initial four and the subsequent four battery modules exceeds 0.2%. The balancing process ends when the working conditions of Ei, Si, and Hi are no longer met.

Figs. 11 and 12 depict the simulation outcomes, while Table 1 provides a consolidated summary of the simulated circuit performance.

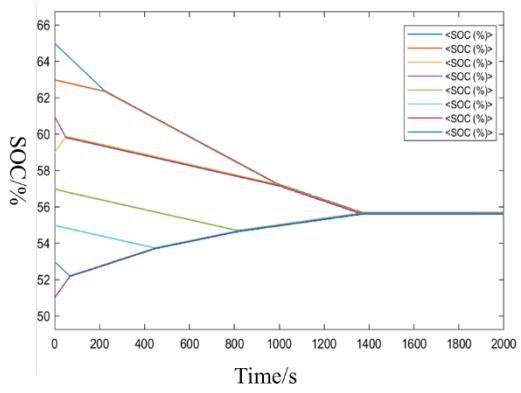

Figure 11. Simulation results of battery pack series equalization topology

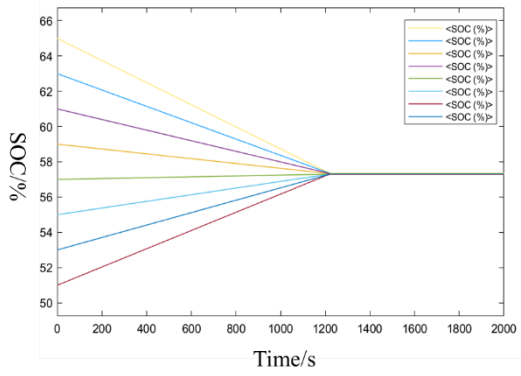

Figure 12. Simulation of hierarchical battery equalization topology

Table 1. Comparison of simulation results for different equalization topologies

	Series equalization topology	Hierarchical equalization topology
Equalization time (s)	1382.57	1220.53
Mean SOC of equalization results (%)	55.65%	57.32%

Variance of equalization results	9.42×10^{-4}	3.43×10^{-4}
Maximum difference of equalization results	0.09	0.06

As summarized in Table 1, the pack with the series equalization topology required 1382.57 s to complete equalization, whereas the pack with the hierarchical topology required only 1220.53 s. This represents an 11.53% reduction in equalization time. Meanwhile, from the maximum error and variance between batteries in the equalized battery pack, simulation results indicate that the hierarchical equalization topology achieves a maximum SOC deviation of 0.06 post-equalization, representing a reduction of 0.03 compared to the series topology; the variance of the hierarchical equalization topology is 0.000343, which is 0.0006 lower than that of the series equalization topology.

Upon analysis of the final equalization results, the battery pack utilizing the series topology exhibits a mean SOC of 55.65%, whereas the pack employing the hierarchical topology achieves a higher mean SOC of 57.32%.

To further verify the superiority of the hierarchical balanced topology, set the simulation DST working condition, where the DST cycle is 12,000 s, the average output current throughout the process is 0.453A, the maximum output current is 4A, and the maximum input current is 2A. The DST cycle includes various states such as battery pack charging, discharging, and rest, thereby replicating the dynamic behavior encountered during actual system operation. Figure 13 depicts the current profile under the specified working conditions, while Figures 14 and 15 present the corresponding simulation outcomes

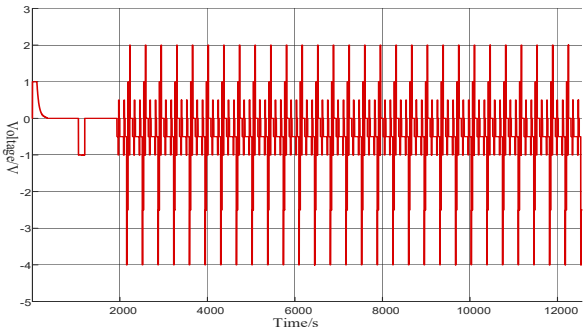

Figure 13. DST operating current waveform

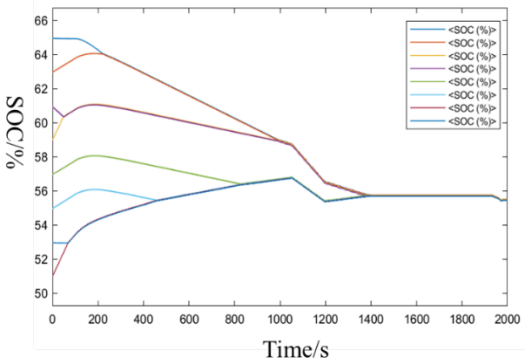

Figure 14. Series topology simulation for DST conditions

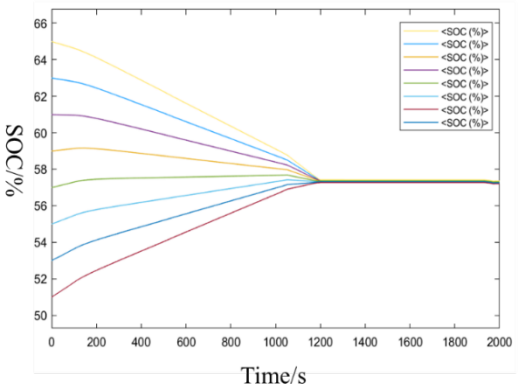

Figure 15. Hierarchical topology simulation for DST conditions

Analysis of the SOC trajectories presented in Figures 14 and 15 reveals that the battery pack's charge/discharge current undergoes continuous fluctuations throughout the equalization procedure, but the SOC values of individual cells always tend to become more consistent. This indicates that the hierarchical equalization topology is more adaptable to the changes of the battery pack under different operating states, which can promote the consistency of individual cells and improve the overall performance.

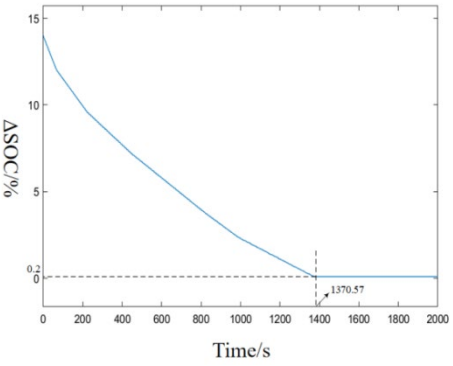

Figure 16. Waveforms of SOC polar variation between cells under series topology

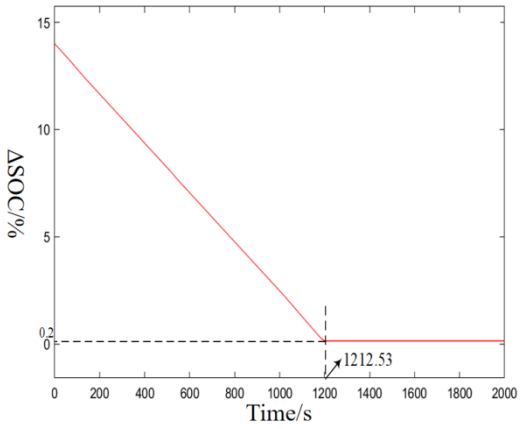

Figure 17. Waveforms of SOC polar variation between cells under hierarchical topology

As shown in Fig.16 and 17, at the moment of equalization activation, the cell-to-cell SOC dispersion within the series-connected battery pack reaches 12.073%. By setting the individual cell range of 0.2% as the equalization end threshold, the series equalization topology requires 1370.57 s to achieve the balancing objective, whereas the hierarchical topology necessitates 1212.53 s, resulting in an 11.53% improvement in equalization speed.

Consequently, the hierarchical topology exhibits reduced energy loss and enhanced energy utilization efficiency compared to the series topology throughout the balancing procedure. The proposed hierarchical architecture outperforms the conventional series-based approach in terms of both balancing velocity and outcome quality.

3. Active Equalization Control Based on Multivariable Fusion Fuzzy Logic

3.1 Analysis of the Equalization Strategy Principle

Effective management of the equalization current requires precise modulation of the MOSFET's duty cycle. The characteristic OCV-SOC curve of lithium batteries presents a challenge: in the high and low SOC regions where the curve is steep, using SOC alone as the control variable can lead to significant current fluctuations and potential over-equalization. Conversely, in the middle SOC plateau region where voltage changes are minimal, reliance solely on voltage can cause misjudgment and prolong the equalization process. Particularly under complex operating conditions, it may trigger erroneous commands. Therefore, in light of the full-state operational characteristics of power batteries, it is irrational to rely solely on voltage or SOC as the sole equalization variable. An in-depth exploration of their coupling relationship is essential. A comprehensive equalization strategy that integrates multiple variables should be considered to evaluate the equalization effect from multiple dimensions.

When considering open-circuit voltage (OCV) and equalization current as the primary factors, the following scenarios typically arise:

1) When the SOC is in the low region, the operating voltage is primarily used to control the equalization current;

2) When the SOC is in the high region, the operating voltage is primarily used to control the equalization current;

3) When the SOC is in the plateau region, SOC serves as the dominant variable for regulating the equalization current;

4) If the charge-discharge current changes slightly, the operating voltage is primarily used to control the equalization current;

5) If the charge-discharge current changes significantly, the operating voltage is primarily used to control the equalization current.

The above scenarios are commonly encountered by the controller. By comprehensively considering other factors, it is necessary to design rule-based strategies applicable to various operating conditions.

Fig.18 illustrates a control scheme based on a Buck-Boost circuit and a multivariable fusion fuzzy equalization strategy. This strategy first calculates the equalization current I_SOC based on SOC deviation and I_V based on voltage deviation through fuzzy control logic for SOC and voltage, respectively. Subsequently, an adaptive fuzzy controller dynamically adjusts the weight C by integrating the battery pack's SOC and charge-discharge current I, fusing I_SOC and I_V to obtain the desired equalization current I0. Finally, a PI controller regulates the MOSFET duty cycle to generate a PWM signal that controls the equalization circuit, enabling the actual equalization current to track I0. This scheme integrates SOC and voltage information to achieve more precise equalization control.

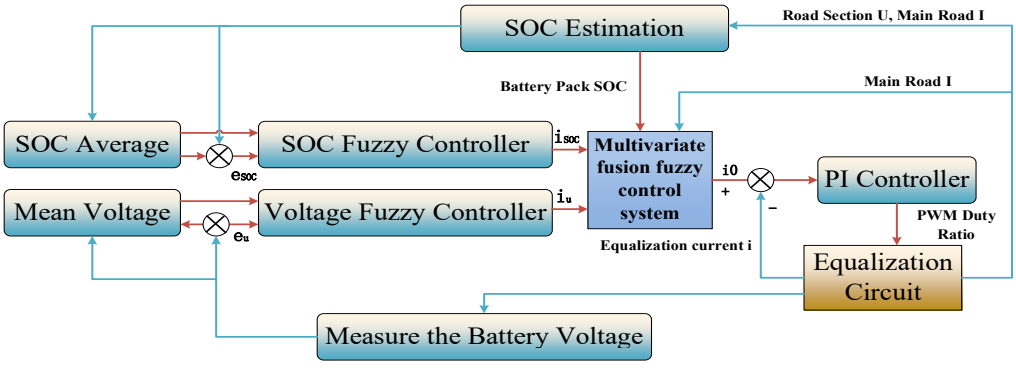

Figure 18. Flowchart of multivariate fusion fuzzy control algorithm

3.2 Design of Voltage and SOC Fuzzy Logic Controller

This study develops a fuzzy controller by incorporating the mean values of voltage/SOC and their deviation e as inputs, and the desired equalization current as the output. The mean values characterize the global condition of the battery pack, while the deviation e governs the equalization speed: large deviations trigger high-current rapid equalization, whereas small deviations activate low-current fine-tuning. This dual-input design ensures both equalization safety (based on mean values) and efficiency (based on deviations).

The fuzzy controller designed in this paper adopts a multivariable input-output structure. The universe of discourse for the SOC mean is defined as [0, 43, 98, 100], while the domain for the average voltage spans [2.5, 3, 3.65, 4.2]. Both employ the fuzzy linguistic variables {L, M, H}, which correspond to low, medium, and high operational states respectively. The domain for SOC deviation is defined as [0, 6.6, 13, 20, 26, 33, 40], while the voltage deviation spans [0, 0.06, 0.13, 0.2, 0.26, 0.33, 0.4]. Both employ the fuzzy linguistic set {NL, NM, NS, Z, PS, PM, PL} to characterize deviation degrees from negative large to positive large. The domain of the output equalization current spans the range [0, 0.6, 1.3, 2, 2.6, 3.3, 4], while employing the same identical fuzzy linguistic variables to characterize equalization currents of varying magnitudes. The specific membership function distributions of all variables are shown in Fig.19.

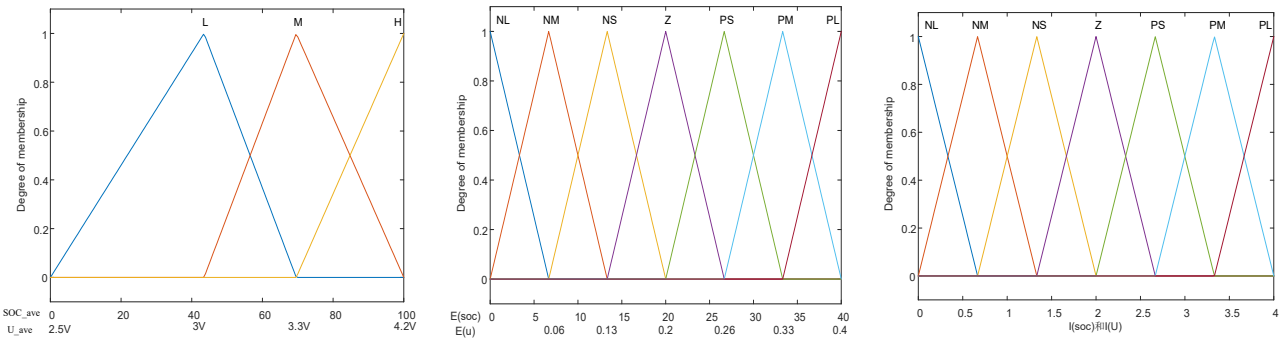

(a)SOC_ave∈[0,100],U_ave∈[2.5V,4.2V] (b) e_SOC∈[0,40], e_U∈[0,0.4] (c)i_SOC, i_U∈[0,4]

Figure 19. Input-output variable affiliation function

Dedicated inference rule bases are constructed for both the State of Charge (SOC) and voltage-based fuzzy controllers. The rule base pertaining to the SOC controller is delineated below:

1) Under the condition where the mean deviation of the State of Charge (e) registers as Negative Large (NL), coupled with a Low (L) global SOC level for the battery pack, the output current I_SOC assumes a value of Negative Small (NS);

2) Under the condition where the mean deviation of the State of Charge (e) registers as Negative Medium (NM), coupled with a Low (L) global SOC level for the battery pack, the output current I_SOC assumes a value of Negative Small (NS);

3) Under the condition where the mean deviation of the State of Charge (e) registers as Negative Small (NS), coupled with a Low (L) global SOC level for the battery pack, the output current I_SOC assumes a value of Negative Small (NS);

4) Under the condition where the mean deviation of the State of Charge (e) registers as Zero (Z), coupled with a Low (L) global SOC level for the battery pack, the output current I_SOC assumes a value of Negative Small (Z);

5) Under the condition where the mean deviation of the State of Charge (e) registers as Positive Small (PS), coupled with a Low (L) global SOC level for the battery pack, the output current I_SOC assumes a value of Positive Small (PS);

6) Under the condition where the mean deviation of the State of Charge (e) registers as Positive Medium (PM), coupled with a Low (L) global SOC level for the battery pack, the output current I_SOC assumes a value of Positive Small (PS);

7) Under the condition where the mean deviation of the State of Charge (e) registers as Positive Large (PL), coupled with a Low (L) global SOC level for the battery pack, the output current I_SOC assumes a value of Positive Small (PS);;

The rule base governing the SOC fuzzy controller is summarized in Table 2:

Table 2. SOC fuzzy controller rule base

i_SOC		e_SOC NL	NM	NS	Z	PS	PM	PL
SOC_ave	L	NS	NS	NS	Z	PS	PS	PS
	M	NL	NM	NS	Z	PS	PM	PL
	H	NL	NM	NM	Z	PM	PM	PL

The rule base of the voltage fuzzy controller is shown in Table 3 below:

Table 3. Voltage Fuzzy Controller Rule Base

i_U		e_U NL	NM	NS	Z	PS	PM	PL
U_ave	L	NS	NS	NS	Z	PS	PS	PS
	M	NL	NM	NS	Z	PS	PM	PL
	H	NL	NM	NM	Z	PM	PM	PL

The fuzzy quantities derived from fuzzy inference cannot be directly applied in practical engineering, as system control variables require precise values. Therefore, defuzzification is necessary to convert fuzzy quantities into precise signals. Common defuzzification methods include: the weighted average method, the bisector method, and the mean of maximum (MOM) method. The weighted average method, also known as the centroid method, calculates the centroid of the area enclosed by the crisp values and their corresponding membership functions, using the former as the x-axis and the latter as the curve. Compared to other methods, it provides smoother control outputs and is easier to implement. The centroid method is employed to defuzzification both the SOC and voltage fuzzy controllers. Their input-output surfaces and fuzzy control simulators are shown in Figures 20-21 below:

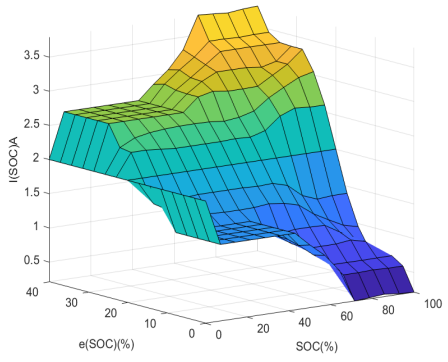

Figure 20. Fuzzy resultant surface plot considering SOC mean and deviation

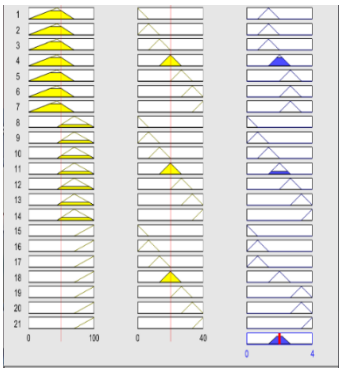

Figure 21. Fuzzy controller simulator considering mean and deviation

3.3 Design of Multivariable Fusion Fuzzy Controller

The operational state of batteries in energy storage systems within smart grids is complex, influenced by multiple factors including state of charge, charge/discharge current, and operating temperature. These factors should be comprehensively considered during battery equalization. The equalization current is synthesized through proportional weighting of the desired current I_SOC generated by the SOC fuzzy controller and the desired current I_V produced by the voltage fuzzy controlle.

$$I0 = C * I\_SOC + (1 - C) * I\_V \quad (13)$$

Where C is the weight obtained from the multivariable fusion fuzzy controller, whose inputs are the overall state of charge (SOC) of the battery pack and the charging/discharging current I, with the weight C as the output variable. Based on experience, the selection of the domain for the primary input variable SOC as [0, 10, 90, 100], while its fuzzy linguistic set employs {L, M, H}, which correspond to Low, Medium, and High levels respectively. Similarly, the universe of discourse for the second input variable charging/discharging current I is selected as [0, 1.6, 3.3, 5, 6.6, 8.3, 10], and its fuzzy language set is defined as {NL, NM, NS, Z, PS, PM, PL}, corresponding to Negative Large, Negative Medium, Negative Small, Zero, Positive Small, Positive Medium, and Positive Large. The universe of discourse for the output variable weight coefficient C is set as {0, 0.25, 0.5, 0.75, 1}, and the fuzzy language set for the output variable C is defined as {B1, B2, B3, B4, B5}. Fig. 22 presents the affiliation functions for both the input and output variables of the weight coefficient fuzzy controller, while Table 4 delineates the corresponding rule base governing the output weight assignment.

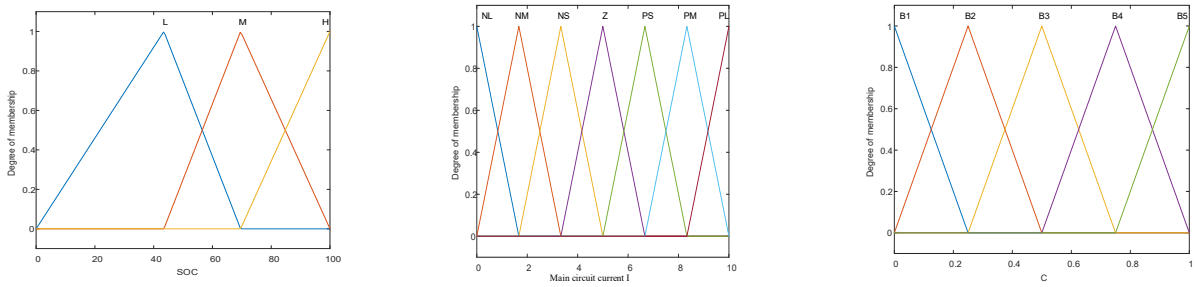

（a）SOC of the battery pack∈[0, 100]　（b）Main circuit current I∈[0, 10]　(c) weight factor C∈ [0, 1]

Figure 22. Affiliation Functions of Input and Output Variables for the Weight Coefficient Fuzzy Controller

Table 4. Rule Base Governing the Weight Coefficient Fuzzy Controller

C		I						
		NL	NM	NS	Z	PS	PM	PL
SOC	L	B1	B2	B2	B3	B2	B2	B1
	M	B5	B5	B4	B4	B4	B5	B5
	H	B1	B2	B2	B3	B2	B2	B1

The fuzzy controller employs the centroid method for defuzzification, and its input-output surface is shown in Fig.23:

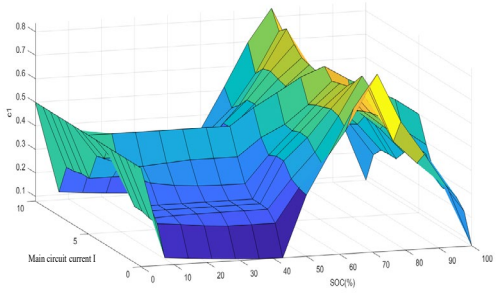

Figure 23. Input-output regular surface plot considering battery charge state and main circuit current output weights

Based on the deviation between the given value and the actual output value, proportional and integral calculations are performed on the deviation, and the control quantity is formed through linear combination to implement PI control on the controlled object. The input signal of the PI controller is the equalization current i0. The PI controller accepts the equalization current i0 as its reference input. Through continuous real-time monitoring, the controller generates an error signal by comparing the commanded equalization current i0 with the measured actual current i within the active balancing branch. The PI controller timely corrects the proportional parameter Kp and integral parameter Ki, generating a control command that acts on the MOSFET to achieve fine adjustment of the equalization current. The PI controller takes i0 output by the multivariable fusion fuzzy controller and the real current i as inputs, and outputs the PWM duty cycle [22].

$$D(k) = K_p \times e(k) + K_i \times \int_0^t e(k)dt \tag{14}$$

Where Kp and Ki represent the proportional and integral parameter values, respectively. e(k) denotes the difference

between the equalization current i0 and the real equalization current i, while D(k) represents the control signal duty cycle [23].

4. Experiments and Results Analysis

To assess whether the balance controller developed in this study satisfies the design specifications of the equalization system, verification was performed utilizing MATLAB/Simulink simulation software. An eight-cell lithium-ion battery equalization simulation framework is built, as shown in fig. 24.

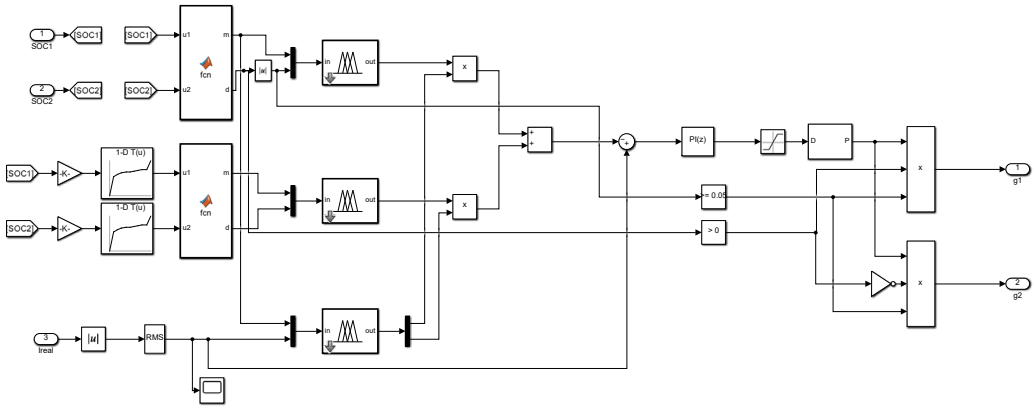

Figure 24. Multivariable fusion fuzzy logic equalization control simulation model

To validate the performance of the proposed strategy under conditions relevant to grid energy storage, this study employs the classical inductor method and single-variable fuzzy control as benchmarks. The evaluation specifically considers the dynamic current profiles and long-term reliability requirements of ESS in smart grids. The eight individual cells within the battery pack are initialized with SOC values set to 65%, 63%, 59%, 61%, 57%, 55%, 51%, and 53% respectively. The simulation outcomes are presented in Figures 25 to 27.

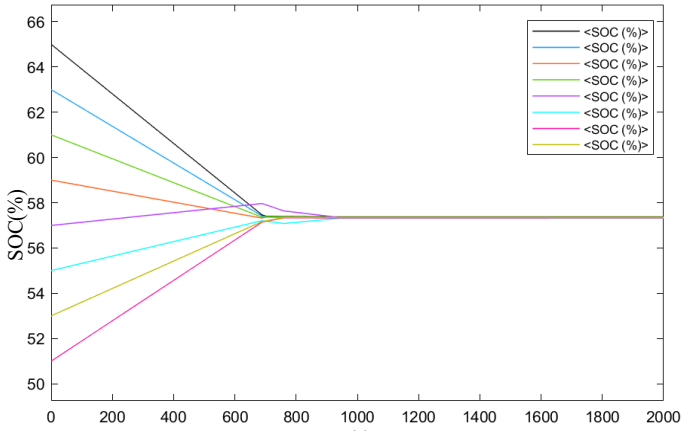

Figure 25. Schematic diagram of equilibrium process based on multivariate fusion control algorithm

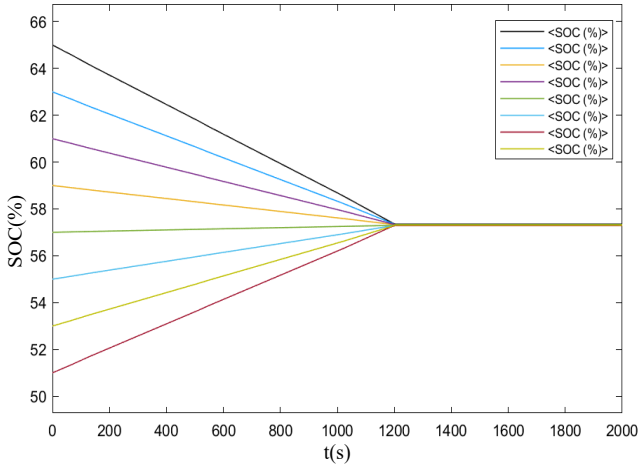

Figure 26. Schematic diagram of the equilibrium process of the classical inductance method

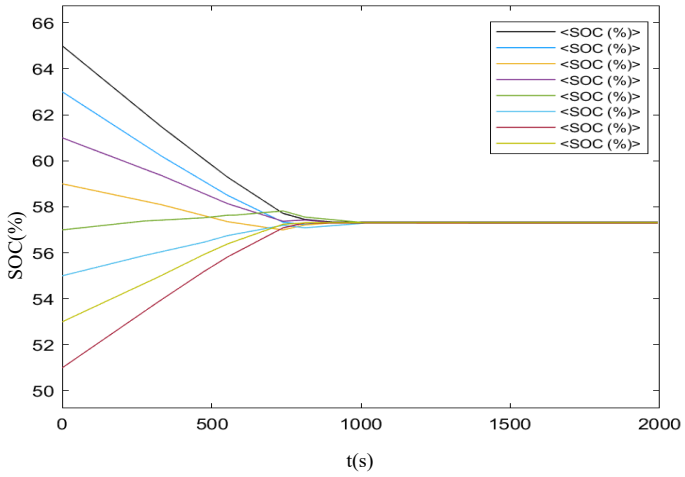

Figure 27. Schematic diagram of SOC-based fuzzy control equalization process

Table 5. Comparison of Equalization Results of Three Algorithms

Algorithm	Equalization Current (A)	Equalization Time (s)	Post-Equalization SOC (%)
Classical Inductor	8	1227s	57.28%
SOC-Based Fuzzy Control	10	1009s	57.32%
Multivariable Fusion	10	906s	57.35%

Comparative analysis of the data presented in Table 5 demonstrates that the multi-variable fusion control algorithm developed in this study achieves a reduction in balancing duration of 26% relative to the classical inductance method and 10% compared to the single-variable control approach. This not only significantly improves the accuracy of battery pack consistency assessment, but also possesses the dual advantages of high efficiency and high reliability.

Among the three comparative algorithms, the classical inductor equalization method exhibits the lowest equalization efficiency, and the time required for it to complete equalization is significantly longer than that of other methods. This limitation primarily stems from its inherent "step-by-step transfer" equalization mechanism, where battery cells can only achieve energy redistribution indirectly through adjacent units. This is specifically manifested as follows: high-SOC batteries must first release energy to adjacent batteries, after which the intermediate batteries transfer the energy to the target batteries. This multi-level energy transfer mode has the following drawbacks: 1) significantly increased

energy transmission path loss; 2) generation of a large number of redundant equalization operations; 3) possible occurrence of repeated equalization phenomena. When a large voltage difference exists between adjacent batteries, this mechanism is prone to triggering safety hazards such as local overcharging, directly threatening the reliability of system operation. The multivariable fusion algorithm proposed in this paper fundamentally circumvents these technical bottlenecks by intelligently optimizing the equalization path and dynamically adjusting the equalization current, significantly enhancing equalization performance while ensuring system safety.

5. Conclusion

To address the state inconsistency in series-connected battery packs for smart grids, this paper proposes a modular hierarchical active equalization architecture. The key contribution is twofold: (1) an improved bidirectional Buck-Boost circuit topology that organizes cells in a hierarchical manner, enabling concurrent intra-group and inter-group energy transfer and overcoming the long, inefficient paths of conventional single-layer topologies; and (2) a multivariable fusion fuzzy logic control strategy that dynamically adjusts the equalization current by integrating both SOC and voltage information, ensuring precise and adaptive control.Comprehensive simulations under various operational scenarios (standby, charging, and dynamic stress test cycles) confirm the effectiveness of the proposed method. The hierarchical topology alone reduces the equalization time by 11.53%. When integrated with the multivariable control algorithm, an additional 26% reduction in equalization time is achieved, leading to a significant mitigation of cell-to-cell inconsistencies and an enhancement in system efficiency and reliability.

While the proposed layered architecture demonstrates superior equalization performance, its implementation in ultra-large-scale systems necessitates a cost-benefit analysis. The increased number of switching components and inductors compared to a simple topology raises the initial hardware cost and control complexity. However, for grid-scale ESS where longevity, reliability, and operational efficiency are paramount, the gains in extended battery pack life and reduced maintenance may justify the initial investment. Future work will include a detailed techno-economic analysis for different system scales.

Acknowledgments.

2025 Zhejiang Province Visiting Engineer Program (FG2025211).

References

[1] Sultan Y A, Eladl A A, Hassan M A, et al. Enhancing electric vehicle battery lifespan: integrating active balancing and machine learning for precise RUL estimation[J]. Scientific Reports, 2025, 14(1).

[2] Wei Y, Dai S, Wang J, et al. Hybrid Natural and Forced Active Balancing Control of Battery Packs State of Charge Based on Partnership for a New Generation of Vehicles[J]. Journal of Electrical and Computer Engineering, 2025, 2018(1).

[3] Zhou H, Xie Y, Li Z, et al. Lithium-ion battery pack equalization: A multi-objective control strategy using interleaved cascaded bidirectional flyback converters[J]. Journal of Renewable and Sustainable Energy, 2025, 17(2):024101.

[4] Liu Y, Meng J, Yang F, et al. A switchable indicator for active balance of the lithium-ion battery pack using a bypass equalizer[J]. Journal of Energy Storage, 2023.

[5] Naguib M, Kollmeyer P, Emadi A. Lithium-Ion Battery Pack Robust State of Charge Estimation, Cell Inconsistency, and Balancing: Review[J]. IEEE Access, 2021, PP(99):1-1.

[6] Di R R, Nicodemo N, Verani A, et al.A novel methodology to study and compare active energy-balance architectures with dynamic equalization for second-life battery applications[J]. Journal of Energy Storage, 2023(Dec. Pt.A):73.

[7] Khan N, Ooi C A, Shreasth, et al. A novel active cell balancing topology for serially connected Li-ion cells in the battery pack for electric vehicle applications[J]. Scientific Reports, 2025,14(1):1-21.

[8] Ouyang Q, Ghaeminezhad N, Li Y, et al. A Unified Model for Active Battery Equalization Systems[J]. Control Systems Technology, IEEE Transactions on, 2025, 33(2):685-699.

[9] Chae C, Noh H J, Lee J K, et al. A High-Energy Li-Ion Battery Using a Silicon-Based Anode and a Nano-Structured Layered Composite Cathode[J].Advanced Functional Materials, 2014, 24(20):3036-3042.

[10] Samanta A, Chowdhuri S. Active Cell Balancing of Lithium-ion Battery Pack Using Dual DC-DC Converter and Auxiliary Lead-acid Battery[J]. Journal of Energy Storage, 2021.33

[11] Sultan Y A, Eladl A A, Hassan M A, et al. Enhancing electric vehicle battery lifespan: integrating active balancing and machine learning for precise RUL estimation[J]. Scientific Reports, 2025, 14(1).

[12] Venkatasatish R, Dhanamjayulu C. Design and implementation of an inductor based cell balancing circuit with reduced switches for Lithium-ion batteries[J]. Scientific Reports, 2024.

[13] Ye Y, Cheng K W E, Yeung Y P B. Zero-current switching switched-capacitor zero-voltage-gap automatic equalization system for series battery string [J]. IEEE Transactions on Power Electronics, 2012, 27(7): 3234-3242.

[14] Shang Y, Xia B, Zhang C, et al. An Automatic Equalizer Based on Forward-Flyback Converter for Series-Connected Battery Strings [J]. IEEE Transactions on Industrial Electronics, 2017: 1-1.

[15] Jing Sun, Dong Dai,An equalization topology based on multi-winding transformer and flyback converter for series-connected lithium-ion battery packs,Journal of Energy Storage[J].,Volume 125,2025,116963.

[16] Ling R, Dan Q, Wang L, et al. Energy bus-based equalization scheme with bi-directional isolated Cuk equalizer for series connected battery strings [C]. 2015 IEEE Applied Power Electronics Conference and Exposition (APEC). 2015: 3335-3340.

[17] Ren H, Zhao Y, Chen S, Wang T. Design and implementation of a battery management system with active charge balance based on the SOC and SOH online estimation [J]. Energy, 2019, 166: 908-917.

[18] Karthikeyan V, Gupta R. Light-load efficiency improvement by extending ZVS range in DAB bidirectional DC-DC

converter for energy storage applications [J]. Energy, 2017, 130: 15-21.
[19] Cai M Y, Zhang E, Lin J, et al. Review on Equilibrium Topologies for Series Lithium-Ion Battery Packs [J]. Proceedings of the CSEE, 2021, 41(15): 5294 5311.
[20] Koseoglou M, Tsiumas E, Jabbour N, et al. Highly Effective Cell Equalization in a Lithium-Ion Battery Management System[J]. IEEE Transactions on Power Electronics, 2020, 35(2):2088-2099.
[21] Duraisamy T, Kaliyaperumal D. Machine Learning-Based Optimal Cell Balancing Mechanism for Electric Vehicle Battery Management System[J]. IEEE Access, 2021, 9(000):16.
[22] Li K, Gao X, Liu C X, Chang C, Li X Y. A novel Co-estimation framework of state-of-charge, state-of-power and capacity for lithium-ion batteries using multi-parameters fusion method[J]. Energy,Volume 269,2023,126820.
[23] Liao L, Li H G, Li H J, Jiuchun Jiang, Tiezhou Wu, Research on equalization scheme of lithium-ion battery packs based on consistency control strategy[J]. Journal of Energy Storage,Volume 73, Part D,2023,109193.
[24] Han, J.; Dong, Y.; Wang, W. Combined Framework for State of Charge Estimation of Lithium-Ion Batteries: Optimized LSTM Network Integrated with IAOA and AUKF. Mathematics 2025, 13, 2590.
[25] S.Hayat, A.Nawaz, Z.Javid, and W.Holderbaum, "Dynamic Load Modelling and Optimised Battery Management Using LSTM for Enhanced Power System Flexibility." The Journal of Engineering2025, no. 1 (2025): e70126.
[26] S. Wang, H. Gao, P. Takyi-Aninakwa, J. M. Guerrero, C. Fernandez and Q. Huang, "Improved Multiple Feature-Electrochemical Thermal Coupling Modeling of Lithium-Ion Batteries at Low-Temperature with Real-Time Coefficient Correction," in Protection and Control of Modern Power Systems, vol. 9, no. 3, pp. 157-173, May 2024.